

HALITE PRECIPITATION AND PERMEABILITY ASSESSMENT DURING SUPERCRITICAL CO₂ CORE FLOOD

Y. Wang^a, T. Luce^a, C. Ishizawa^a, M. Shuck^a, K. Smith^a, H. Ott^b, and M. Appel^a
Shell International E & P, Inc., a – USA, b – The Netherlands

This paper was prepared for presentation at the International Symposium of the Society of Core Analysts held in Halifax, Nova Scotia, Canada, 4-7 October, 2010

ABSTRACT

We present an experimental study of halite precipitation and permeability impairment on Berea core during supercritical (SC) CO₂ core flood, specially aiming at identifying and quantifying post-flood dry zones and permeability changes, respectively on the core after CO₂ exposure. The flood experiments were performed on brine saturated Berea cores of 1.5 inch diameter and 1 foot length. Pressure side taps were included to monitor pressure profiles, and evaluate permeability changes along the core during different stages of the experiment. Magnetic Resonance Images (MRI) were taken on the core after the flood. Permeability calculated from pressures indicates a dry zone near the injection side and shows that CO₂ effective permeability after flood at the remaining water saturation (S_{wf}) is roughly half of the expected value from a similar core without CO₂ exposure at same S_{wf} . With the aid of MRI technique, the dry zone and saturation profiles are confirmed to be consistent with the pressure measurements. A qualitative explanation of the observations based on SC CO₂ – brine – rock interaction is presented.

INTRODUCTION

In the carbon capture and storage (CCS) study, deep saline formation has drawn more and more attention because of its wide availability and potentially large storage capability. As dry carbon dioxide (CO₂), usually in supercritical (SC) phase, is injected into highly saline formations, a variety of coupled physical and chemical processes happen at different CO₂ saturation [1, 2]. Those processes include but are not limited to the advection-dominated immiscible displacement of aqueous phase by CO₂ phase, dissolution of CO₂ into the aqueous phase, and water evaporation. Chemical interaction may also occur between aqueous CO₂ and primary aquifer minerals.

Among those processes, water evaporation can potentially dry out a formation and cause the precipitation of halite. Deposition of halite scale has been observed in gas storage wells in the Netherlands and Germany [3]. In the proximal well bore area where the CO₂

flow rate is the highest, halite precipitation and formation dry out may impact the permeability and injectivity. Theoretical study has been performed and predicted the permeability impairment and potential loss of injectivity during CO₂ injection into both saline aquifers [1, 4], and depleted gas reservoirs [5, 6]. On the other hand, little experimental result has been reported.

In 2008, we started series of core flood experiments to study the halite precipitation during SC CO₂ injection. In previous work [7], salt crystals were observed inside the core along the CO₂ flow direction. Pressure drop across the core after the CO₂ flood suggested a permeability reduction. In this paper, we present our progress in this study with aids of pressure profile measurement and magnetic resonance imaging (MRI). We chose the similar experimental parameters, and compare results from this work with what previous reported, with an emphasis on the permeability assessment and dry out zone identification.

EXPERIMENT

The experimental setup was similar to that described in Ref. [7]. We also followed the same procedure to prepare the core assembly. A major improvement was the measurement of pressure profiles along the core by 6 side taps, at ~ 5 cm spacing (Figure 1). The Berea core used in this work was 11.52 inches long (29.25 cm) with the diameter of 1.49 inches (3.791 cm). Its pore volume (PV) was measured as 57.5 cc, corresponding to a porosity of 17 %. CO₂ used in this experiment was dry with water content less than 2 ppm. For the core flood experiment, the dual injection pumps were charged with liquid CO₂ at room temperature of 22 °C and injected continuously at a rate of 2.66 cc/min. The density and viscosity of CO₂ were 0.814 g/cc and 0.073 cP, respectively. The core holder with pressure side taps, back pressure regulator (BPR), inlet and outlet pressure transducers were all enclosed in an oven at 50 °C. Pore pressure in the core was set by BPR and was about 1203 psi. During the entire injection, BPR pressure varied between 1195 psi and 1204 psi due to small temperature fluctuation in oven. Inside the oven, CO₂ density was 0.236 g/cc, and the viscosity was 0.021 cP. From the density contrast, the actual CO₂ injection rate into the core was about 9.2 cc/min.

The procedure is briefly outlined below. After cleaning and oven drying, the Berea core was sleeved and loaded into the core holder. An effective confining stress (i.e. absolute confining pressure minus injection pressure) was applied on the core at 1000 psi. Gas permeability was measured by the steady state method using both N₂ and CO₂ at room temperature. The core was then vacuumed and saturated with brine of 25 wt% sodium chloride (NaCl) by a pump. Both pore volume and dead volume were measured from the pump volume change. Steady state brine permeability was measured on the fully saturated core. Oven temperature was then elevated to 50 °C and stabilized over night. Thereafter, pump started injecting dry SC CO₂ into the system. SC CO₂ first bypassed the

core holder for about 10 minute, and then flowed into the core. The injection was continued for about 19 hours until liquid production ceased and the pressure drop across the core was constant. Produced fluid including both liquid and water vapor flowed through BPR first and then was collected by two traps. After the injection had been stopped, the oven temperature was decreased back to room temperature. Steady state CO₂ gas permeability was measured again on the Berea core with the remaining brine saturation (S_{wf}). When all the permeability measurements were finished, the core assembly was unloaded and weighed to determine S_{wf} by mass balance. The core was kept sleeved until it was ready for MRI scans. MRI images were taken along the core in 8 different zones. For comparison purposes, MRI image was also taken on another Berea core fully saturated with brine of the same salinity but without being CO₂ flooded.

It worth pointing out that accuracy of pressure reading from transducers was very important. It directly affected the pressure drop measurements, thus impacted the permeability assessment greatly. In the experiment, pressures at core inlet, outlet, side taps, and BPR were measured by Heise DXD transducers with an accuracy of $\pm 0.02\%$ at full range of 2000 psi. The offsets (ΔP_0) between transducers were first measured at the end of CO₂ gas permeability measurement. When gas flow was stopped and pore pressure was slowly decreased down to atmospheric pressure, zero shift on each transducer was obtained by averaging its reading for 5 min. The result was used in the permeability calculation. Drifts in ΔP_0 due to changes in pressure and temperature were evaluated at the beginning of injection while SC CO₂ was bypassing the core, the pore pressure was stabilized around 1098 psi. ΔP_0 between transducers at inlet and side taps were recorded. The transducer at core outlet was not isolated from the bypass flow, so the drift in outlet pressure reading could not be estimated.

RESULTS AND DISCUSSION

Core Flood

In total, about 176 PV of SC CO₂ was injected into the core. At the beginning of the injection, pressure drop across the core (ΔP) built up to 24 psi quickly. The breakthrough of SC CO₂ happened at about 0.3 PV of injection. After the breakthrough, ΔP decreased down to around 2.1 psi. About half of the total produced brine was collected around the time of breakthrough. The brine production was greatly slow down after the breakthrough and stopped after about 150 PV of SC CO₂ being injected. In contrast, vapor production increased linearly with time at a rate of 1.1 g/hr during the first 4 hours. After that, vapor production slowed down. If approximated by another linear trend, the rate was about 0.58 g/hr. The decrease in the evaporation rate was also observed in other core experiment flowing with dry methane [8]. More discussion on vapor production as function of time will be found in the section of “SC CO₂ – Brine Interaction”.

Remaining Water Saturation

Remaining water saturation (S_{wf}) was determined using fluid production and mass balance. Total fluid production was 39.38 g or 42.05 cc including the mobile water in the core (33.54 cc) and the water in tubing and dead volume of pressure transducers (about 8.51 cc). Pore volume of the Berea core was 57.5 cc, so S_{wf} was 42%. As there were uncertainties in estimating brine production from dead volume of pressure transducers, estimated uncertainty in S_{wf} by production was 6%, so that $S_{wf} = (42 \pm 6)\%$. On the other hand, compared with the dry weight, the core after CO₂ flood gained a weight of 36.86 g. From the weight gain, S_{wf} was calculated to be 47%; higher than the actual value due to excess weight from the remaining brine and precipitated salt. S_{wf} from two methods agreed well with each other.

Permeability Assessment

In all the permeability calculation, measured ΔP had been corrected for the offset ΔP_0 . Between inlet and outlet, $\Delta P_{0_{io}} = -0.1$ psi. Before the flood experiment, Klinkenberg permeability (k_{abs}) on the dry, clean Berea core was around 240 mD (237 using N₂ gas and 244 mD using CO₂ gas). Uncertainty in gas permeability measurements was about ± 20 mD. The brine permeability (k_w) was 143 mD using ΔP between inlet and outlet. The uncertainty was about ± 5 to ± 10 mD. The above uncertainties in both gas permeability and brine permeability were estimated based on the measurements at different flow rates. Pressure response from individual side taps were also used to check the brine permeability in the core between taps (Figure 2 (a)). Within measurement uncertainties, brine permeability was approximately the same across the core, indicating that the core was reasonably homogeneous. Table 1 summarizes the permeability measurements in this work.

During the last couple of hours of the injection, ΔP across the core was stabilized at 2.1 psi. ΔP was contributed by SC CO₂ flow, as the liquid production stopped and remaining brine was immobile. For the final 6 PV of injection, the average pressures were: 1204.2 psi at inlet, 1203.2 psi at T1, 1203.1 psi at T3, 1202.9 psi at T4, and 1202.1 psi at outlet. Unfortunately, the rest of side taps were plugged by precipitated salt during the injection. Using the above measured pressures, SC CO₂ permeability was calculated to be 58 mD between inlet and outlet. Permeabilities from side taps are illustrated in Figure 2 (b). Where ΔP_0 used for ΔP correction were: $\Delta P_{0_{io}} = -0.1$ psi, $\Delta P_{0_{i1}} = 0.1$ psi, $\Delta P_{0_{13}} = -0.2$ psi, $\Delta P_{0_{34}} = 0.1$ psi, and $\Delta P_{0_{4o}} = -0.1$ psi. Note that the above offsets were measured at ambient condition. At 1098 psi and 50 °C, offsets between inlet – T1, T1 – T3, and T3 – T4 were measured as 0.1 psi, -0.4 psi, and 0.4 psi, respectively. It showed that offsets $\Delta P_{0_{13}}$ and $\Delta P_{0_{34}}$ varied as pressure and temperature increased, and $\Delta P_{0_{i1}}$ was more stable.

Based on the accuracy of transducers and offsets between them, uncertainties in those permeabilities from side taps could be larger than that from inlet and outlet pressures. It was because that ΔP between side taps was smaller than that between inlet and outlet, and

was impacted by ΔP_0 more seriously. As for permeabilities between side taps, given the variations in ΔP_{0_13} and ΔP_{0_34} , uncertainties in the permeabilities from T1 – T3 and T3 – T4 were larger than that from inlet – T1. With the above uncertainty analysis, pressure measurement suggested that core close to the inlet side was greatly impacted, thus the permeability dropped dramatically.

CO₂ Klinkenberg permeability (k_{eg}) on the core after flood at S_{wf} and room temperature was 89 mD between inlet and outlet. The ratio of k_{eg} and k_{abs} (= 244 mD) was 0.365 (Figure 3). Also shown in the figure are the ratio from previous work [7], and the gas relative permeability (k_{rg}) curve on a Berea core plug with similar properties but without SC CO₂ exposure. In both experiments, k_{eg}/k_{abs} reduced to a similar value at similar S_{wf} . When compared with the expected value, i.e. k_{rg} at the same S_w , this ratio was roughly half. Error bars demonstrate the uncertainties in k_{eg} (Figure 3). For S_{wf} , error bars show the uncertainty in S_{wf} , i.e. $\pm 6\%$, whereas for k_{eg}/k_{abs} , error bars give the range of possible values from least to most favourable. For example, the least favourable was calculated assuming that k_{eg} was 20 mD higher than the actual values, and k_{abs} was 20 mD lower than the actual value ($k_{eg}/k_{abs} = 74/259 = 0.286$). From the figure, even with uncertainties considered, k_{eg}/k_{abs} was still lower than the expected value by a factor of 1.6 – 2.6.

Note that depending on which absolute permeability was used, ratio k_{eg}/k_{abs} was not necessarily the relative permeability. In the above discussion, k_{abs} on the dry, clear core was used to illustrate the reduction in effective permeability. A true k_{rg} would be obtained if k_{abs} on the core after CO₂ flood had been measured and used. From its definition, the measured reduction in the effective permeability was due to two possible reasons: one was the higher brine saturation so that lower k_{rg} ; and the other one was the reduction in k_{abs} due to the precipitated salt. MRI was used to study the brine saturation.

Magnetic Resonance Imaging (MRI)

18 MRI images were taken on core slices in 8 different zones along the core post-flood (Figure 4). Figure 5 shows some of those MRI images, and Figure 6 shows an image of a Berea core fully saturated with 25 % brine and without being CO₂ flooded. All MRI images had been normalized so that the average background in each image was at the same noise level. With that normalization, the brightness in each image was proportional to the amount of fluid in the scanned region, and was directly comparable to other images. In a fully saturated core, all the pore space was saturated with brine. In comparison, in the core after being CO₂ flooded, $S_{wf} = 0.42$. 58% of the pore space was filled with CO₂ and a certain amount of precipitated salt, which did not contribute to the resonance. Therefore, stronger signal and sharper contrast were observed in Figure 6. Images in Figure 5 were darker. Among those images in Figure 5, image from the Slice (a) was close to the inlet end, about 0.9 cm into the core, image from the Slice (f) was close to the outlet end, about 0.2 cm away from the end, and images from Slices (b – e) were taken along the core between inlet and outlet ends. Images from closer to the core inlet were darker than those from near the outlet, suggesting that in the core after flood, the inlet side was drier than the outlet. The dark area on the Slice e may indicate a local

dry spot. The bottom and right edges on the Slice f were darker than rest of the area; probably due to the additional drying by air when images were taken.

Brine saturation distribution $S_w(x)$ was calculated from those images. In the calculation, a constant threshold value was chosen to account the resonance signal in each image. The resonance signal from each image was proportional to the brine saturation over the corresponding slice in the core. When the resonance signal was plotted as a function of slice location, it represented the brine saturation distribution profile along the core (lower portion of Figure 4). In the figure, the saturation profile was normalized so that the average saturation over the core (i.e. the area under saturation profile curve) was 42 %. From the profile, S_w at inlet end was much lower and increased gradually towards the outlet end.

MRI measurement showed that the inlet side of the core was much drier than the other part. Combined with the above permeability assessment, the measured reduction in effective permeability was due to the decrease in the absolute permeability, which was caused by the precipitated salt. In particular, the SC CO₂ permeability between inlet and T1 dropped down to ~15 mD. It suggested that more salt precipitated near the inlet end and reduced the permeability.

SC CO₂ – Brine Interaction

Results from both pressure profile measurements and MRI images suggested that a “dry zone” developed near the core inlet side during the dry SC CO₂ injection. In the dry zone, brine saturation was much lower and the permeability dropped greatly due to plugging from the precipitated salt. Salt precipitation was caused by water evaporation from brine to SC CO₂.

While a detailed theoretical study using geochemical reactive transport modeling is needed and ongoing, a conceptual model can be used to describe the SC CO₂ – brine interaction (Figure 7) [9]. As dry CO₂ is injected into a brine saturated core, in addition to the brine displacement by CO₂ and CO₂ dissolution into the brine, water is evaporated and carried by CO₂ flow to the downstream. When pressure drops, water vapor absorbed in CO₂ condenses. This water condensation dilutes the brine. Therefore, halite precipitates near the core inlet side, rather than further inside the core. Moreover, in a core flood experiment, besides the forward flow of CO₂-rich phase, there is another backward aqueous flow. When displacing brine with gas in a core, capillary end effect works as a barrier that prevents the brine outflow from the core. Imbibition occurs because of the capillary pressure gradient. The imbibition brings brine back towards the core inlet. The evaporation continues when the brine backflow meets the injected dry SC CO₂, which may potentially increase the local salt accumulation due to the precipitation. This capillary driven back flow has also been modeled in Ref. [6] to explain the salt precipitation in CO₂ injection. On the other hand, as brine salinity increases due to the water evaporation, water activity in brine decreases, so does the evaporation. The water activity is defined as the vapor pressure of liquid divided by that of pure water at the

same temperature. It is a function of chemical components in the liquid. Water evaporation will stop totally when the water activity in brine equals the relative humidity in CO₂ gas phase. In this experiment, vapor production did not seem to follow this prediction. However in the later stage of injection, the vapor production was probably due to the evaporation of produced brine, as the produced vapor passed the liquid trap first before collected by vapour trap. Indeed, volume decrease of ~3 cc in produced brine was observed during experiment. Therefore recorded vapor production, especially at the later time, did not represent the true vapor production from the core.

CONCLUSION

During CO₂ injection into a saline formation, permeability impairment due to halite precipitation is an important aspect. In this work, a core flood experiment showed that when SC CO₂ was injected in a brine saturated core sample, a dry zone near the core inlet side developed and salt precipitated. The dry zone was indicated by both pressure profile measurement and MRI images. At the end of core flood, gas phase effective permeability at S_{wf} dropped approximately by a factor of 2. The precipitation was the result of water dissolving into the SC CO₂. A conceptual model was used to describe the SC CO₂–brine interaction. More research is planned for better modeling the core flood experiment and correctly applying its results to a reservoir scale.

ACKNOWLEDGEMENTS

We thank Guoxiang Zhang, Zheyi Chen and Daniel Sturmer for insightful discussions. We are grateful to the Shell International E & P, Inc. for the permission to publish this manuscript.

REFERENCES

1. Pruess, K. and Garcia, J., “Multiphase Flow Dynamics during CO₂ Injection into Saline Aquifers”, *Environmental Geology*, **42**, 282 (2002).
2. Pruess, K. and Spycher, N., “ECO2N – A fluid property module for the TOUGH2 code for studies of CO₂ storage in saline aquifers”, *Energy Conversion and Management*, **48**, 1761 (2007).
3. Kleinitz, W., Koehler, M., and Dietzsch, G., “The precipitation of salt in gas producing wells”, *SPE* 68953, (2001)
4. Hurter, S., Labregere, D., and Berge, J., “Simulations for CO₂ Injection Projects with Compositional Simulator”, *SPE* 108540-MS, (2007)

5. Giorgis, T., Carpita, M., Battistelli, A. and Marzorati, D., “Modeling brine evaporation and halite precipitation driven by CO₂ injection in depleted gas reservoirs”, *8th International Conference on Greenhouse Gas Control Technologies (GHGT-8)*, Trondheim, Norway, (June, 2006).
6. Carpita, M., Giorgis, T., and Battistelli, A., “Modeling CO₂ Injection with Halite Precipitation using an Extended Verma & Pruess Porosity – Permeability Model”, *Proceedings, TOUGH Symposium 2006*, LBNL (May, 2006).
7. Wang, Y., Mackie, E., Rohan, J., Luce, T., Knabe, R., and Appel, M., “Experimental Study on Halite Precipitation during CO₂ Sequestration”, *SCA Proceedings 2009-25* (2009).
8. Grattoni, C., Guise, P., Phillips, G. Fisher, Q., and Knipe, R., “Evaluation of Water Evaporation and Salt Precipitation due to Flow in Gas Reservoirs”, *SCA Proceedings 2009-14* (2009).
9. Zhang, G., Taberner, C., Cartwright, L., and Xu, T., “Injection of Supercritical CO₂ into Deep Saline Carbonate Formations. Predictions from Geochemical Modeling”, *SPE journal*, (in press).

Table 1: Summary of Measured Permeability on the Berea Core

Permeability Measurements on Berea Core	K (mD)
N ₂ gas Klinkenberg permeability on dry clean core	237
CO ₂ gas Klinkenberg permeability on dry clean core	244
Brine permeability on fully saturated core	143
SC CO ₂ Permeability on the core flood at S_{wf}	58
CO ₂ gas Klinkenberg permeability on the core post-flood at S_{wf}	89

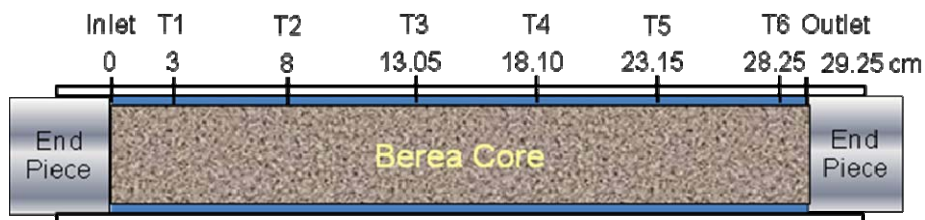
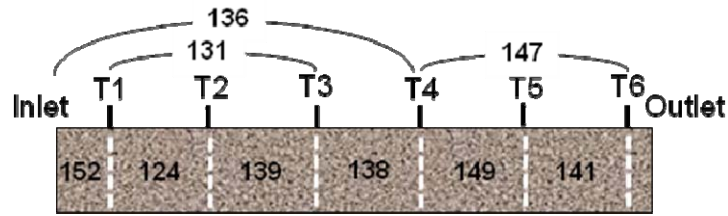
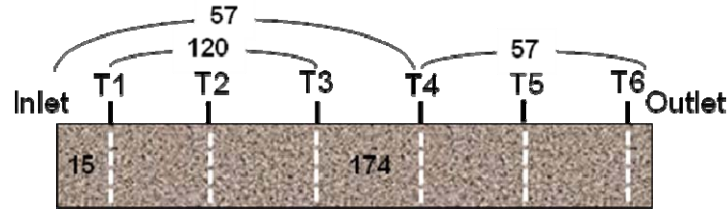


Figure 1: Core assembly and locations of pressure side taps.



(a)



(b)

Figure 2: Permeability of the Berea core. (a) Brine permeability (mD) inside the core between side taps before CO₂ core flood. (b) SC CO₂ permeability (mD) from pressure side taps during the final 6 PV of SC CO₂ injection.

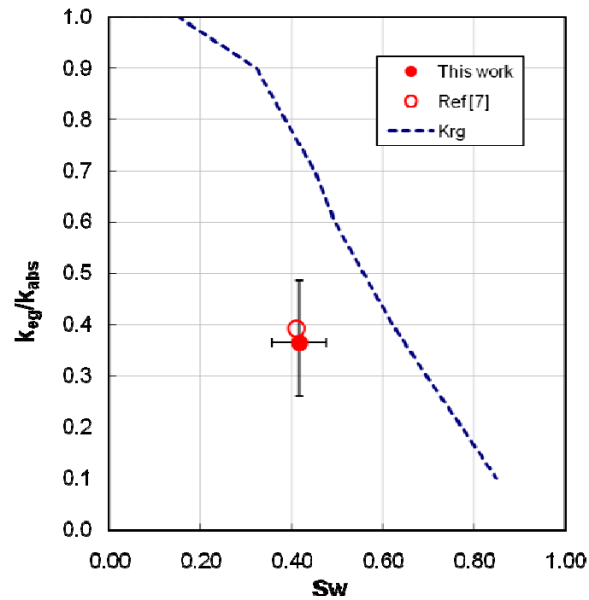


Figure 3: Comparison between k_{eff}/k_{abs} at S_{wf} of the Berea core after SC CO₂ core flood and that of a Berea core without being CO₂ flood. See text for explanation.

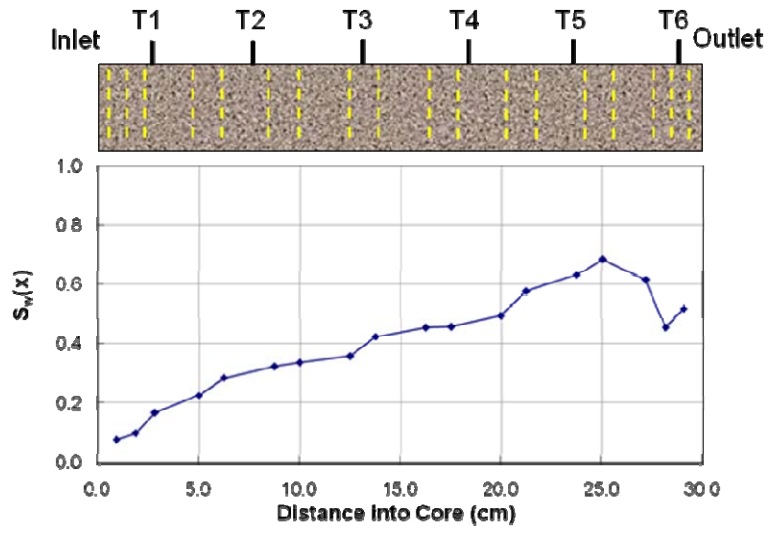


Figure 4: Top: schematic of slice locations (in yellow dash line) where MRI images were taken. Bottom: saturation profile along the core after CO₂ flood.

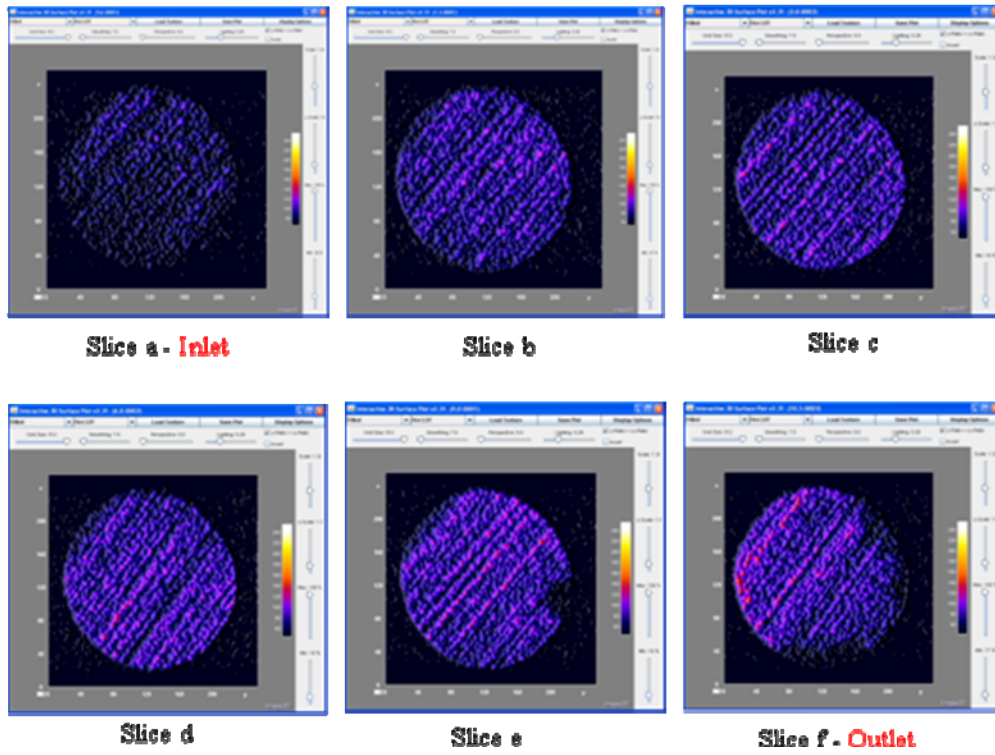


Figure 5: MRI images on the core after SC CO₂ flood.

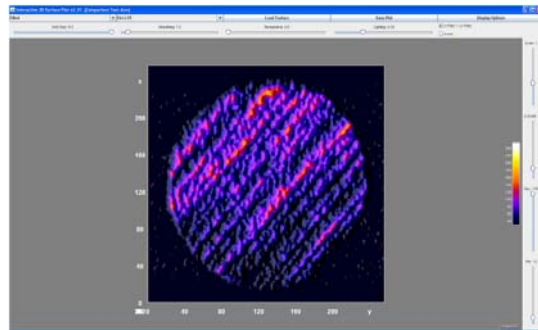


Figure 6: MRI image on a Berea core fully saturated with 25 % brine, and no CO₂ flood.

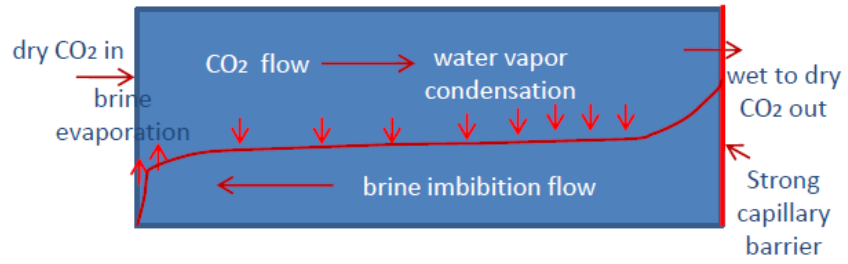


Figure 7: A conceptual model of CO₂ – brine interaction during CO₂ injection.